Growth of nano-tendril bundles on tungsten with impurity-rich He plasmas

To cite this article before publication: Dogyun Hwangbo *et al* 2018 *Nucl. Fusion* in press https://doi.org/10.1088/1741-4326/aacd1f

Growth of nano-tendril bundles on tungsten with impurity-rich He plasmas

Dogyun Hwangbo[1], Shin Kajita[2], Noriyasu Ohno[1], Patrick McCarthy[3], James W. Bradley[3] and Hirohiko Tanaka[1]

[1] Graduate School of Engineering, Nagoya University, Furo-cho, Nagoya 464-8603, Japan
[2] Institute of Materials and Systems for Sustainability, Nagoya University, Furo-cho, Nagoya 464-8603, Japan
[3] Department of Electrical Engineering and Electronics, University of Liverpool, Brownlow Hill, Liverpool, L69 3GJ, UK

E-mail: hwangbo@nagoya-u.jp

Abstract
Isolated regions of nano-tendril bundles (NTBs) have been grown on tungsten surfaces exposed to low-pressure direct-current (DC) helium plasma discharges operating with the addition of impurity gases, including neon, argon, nitrogen and residual air. Through the variation of impurity gas partial pressures and bombarding ion energies, threshold conditions and operational ranges for the growth of NTB's have been investigated. It was found that increasing the vacuum base-pressure from ~10^{-5} to ~10^{-4} Pa during the experiment could give rise to NTB formation without the need for other additional gases. In general, the required impurity gas ratio and the incident ion energy necessary to form these structures was found to vary across the range of different additional gas species, with a key parameter being the net erosion yield (Y) due to ion bombardment, $Y \sim 10^{-2}$–10^{-3}, with the morphology altering with changing net erosion yield. It is predicted that erosion-deposition processes acting upon existing He-induced morphology changes are the precursors for NTB growth.

Keywords: helium, tungsten, plasma wall interaction, nanotendril, fuzz, sputtering

1. Introduction

The combined presence of eroded plasma facing component (PFC) material, seeded impurity gases, hydrogenic plasma and helium (He) ash in the divertor region of a fusion device make the plasma surface interactions within these regions very complex. In terms of operation of a fusion device the performance of divertor materials, both under steady state and high energy transient event conditions, is a critical issue and has been recognized as an important topic in plasma-surface interaction research. Helium has been well known to interact with tungsten (W), which is a candidate material for divertor regions of future fusion devices like ITER and DEMO owing to its excellent refractory and electrical properties [1, 2]. He-W interactions have been studied actively through laboratory experiments [3–6], and those studies have revealed that the morphology of a W surface could be significantly changed with He ion exposure. Helium bubble formation [3] is an example of those changes and is also known to be intrinsically related to the formation of fibre-form nanostructure, which consists of numerous entangled nanoscale tendrils, so-called W 'fuzz' [4–6]. Since fuzz formation was first observed, the formation conditions have been investigated [6], and the considerable changes in thermal and electrical properties have been revealed [7–10], which may greatly affect interactions between plasma and W surfaces.

Recently, a new morphology change, nano-tendril bundles (NTBs) was reported by *Woller et al.* These are isolated 'islands' of bundles of nanostructures which could grow up to 100 times taller than typical fuzzy layer thickness of several μm [11]. In their report the surface was not fully covered with NTBs whereas fuzz has been seen to more uniformly cover the full area of a W surface upon which it forms. *Woller et al* used 13.56 MHz radio frequency (RF) modulated He plasma, with an ion energy distribution of 30–100 eV, to produce the NTBs and revealed an approximate temperature window for formation of NTB in the range of 870–1220 K [11]. The upper temperature boundary is less than that for fuzz formation while the lower boundary was similar [6].

For ITER and DEMO heat-load mitigation using impurity gas seeding is considered to protect divertor plates in standard operation campaigns [12, 13]. Thus, it is of importance to reveal possible effects of impurity ion irradiation on the morphology change of W surface. In this paper, we show the formation of NTBs using impurity-rich He DC plasma irradiations, without RF modulation. The effect of changing gas impurity type, its concentration in the plasma and the

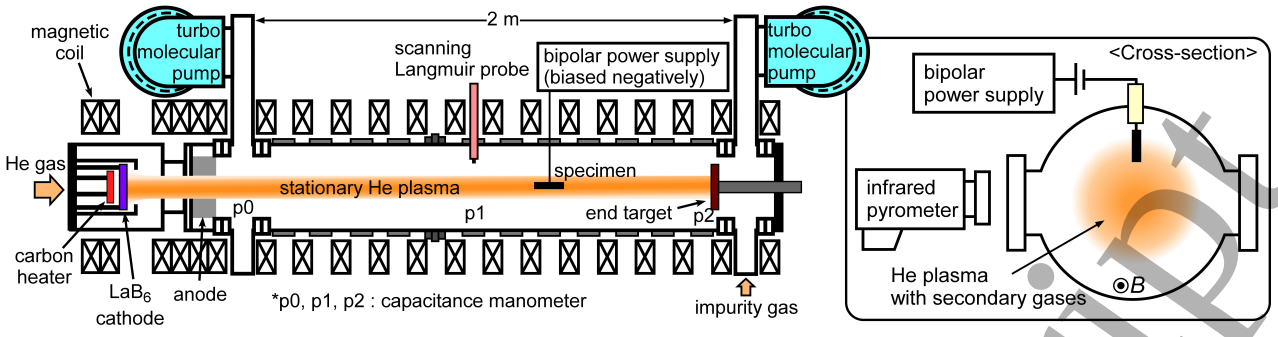

Figure 1. Schematic of the NAGDIS-II plasma experiment. The right figure shows the cross-section of the vacuum chamber viewed from the downstream.

incident ion energy on NTB structures formation is investigated, and the surfaces were characterized using scanning electron microscope (SEM) techniques.

2. Experimental methods

Experiments were conducted in the linear magnetized plasma device NAGDIS-II (NAGoya DIvertor Simulator), which can produce a high density plasma by DC discharge using a LaB_6 cathode heated by a carbon heater [14]. Figure 1 shows a schematic of the experiment. Helium plasma was produced along the magnetic field of 0.1 T, and the typical electron density and temperature were ~10^{19} m^{-3} and ~5 eV, respectively. Thin W samples (5 or 10 × 10 × 0.2 mm^3, 99.95%, PLANSEE) were installed ~1.4 m away from the plasma source oriented parallel to the magnetic field line; the surface normal was perpendicular to the magnetic field. The sample was biased negatively via a power supply to control the incident ion energy in the range of 50–500 eV. During the plasma exposure, the surface temperature was measured using an infrared pyrometer with 1.6 μm wavelength and the emissivity was set to 0.3. The surface temperature was initially fixed to a specific value for each sample and decreased gradually as the surface became black in the case that a fuzzy layer was formed. Significant non-uniformity in temperature did not exist on the surface, whereas there existed +/-10 K of measurement error on any temperature measurement. The temperatures in the experiment were in the range of 1100–1600 K, which was higher than the NTB's formation window identified in the work by *Woller et al* [11], within the range of fuzz growth [6], and the incident ion flux and fluence varied in the range of 0.2–2 × 10^{22} $m^{-2}s^{-1}$ and 0.7–6 × 10^{25} m^{-2}, respectively.

In this experiment, the impurity level in the He plasma was an important parameter. It was controlled using two methods: 1) increasing the background vacuum level and 2) injecting secondary gas. To vary the background pressure, a gate valve, connected to a turbo-molecular pump mounted at the downstream region of the NAGDIS-II device, was opened and closed. This allowed the background pressure to be varied from ~8 × 10^{-5} to ~3 × 10^{-4} Pa. Preliminary experiments using spectroscopy [15] and mass spectrometry revealed that the main components of the background gases were nitrogen (N_2) and oxygen (O_2). When conducting the secondary gas injection experiments, the background pressure was maintained at ~8 × 10^{-5} Pa by two turbo molecular pumps, with primary He gas being inserted from the upstream and secondary gases, nitrogen (N_2), argon (Ar) and neon (Ne), seeded from the downstream of the device. Gases were introduced into the system using mass flow controllers, at a constant He flow rate of 200 sccm. The flow rates of the secondary gases were changed to alter the impurity concentration in the plasma each time. The impurity gas ratio (the partial pressure to the total pressure) was determined using interpolation between the two neutral gas pressure values, which were measured by two capacitance manometers located at 30 cm upstream and 60 cm downstream of the sample position, as shown in figure 1. The operational pressure was varied in the range of 0.7 to 0.8 Pa by changing the secondary gas concentration. To evaluate the net erosion yield, the samples were weighed before and after the plasma exposure using an electronic scale (A&D Co., BM–22) with a precision of 1 μg. Masses measurements were made ten times for each sample (both pre and post irradiation) and then an average was taken. After the plasma exposure, the morphology of NTBs and neighboring surfaces were investigated using SEM observation.

3. Results and Discussion

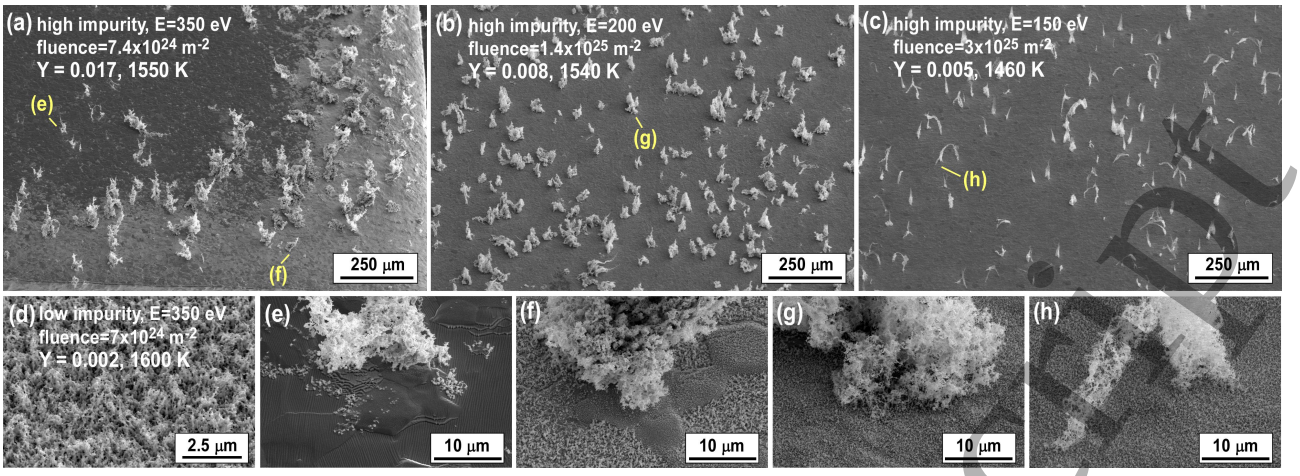

Figure 2. The SEM micrographs of nano-tendril bundles on tungsten samples viewed at 45° from the normal. (a)–(c) show the NTBs with the background pressure of ~10^{-4} Pa at different incident ion energies: (a) 350, (b) 200 and (c) 150 eV. (e)–(h) shows enlarged micrographs of the bottom of NTBs at the positions presented with marks in (a)–(c). (d) shows the fuzzy nanostructure with the background pressure of ~10^{-5} Pa.

3.1 NTB growth with increase of background vacuum level

Figures 2(a)–(c) show the SEM micrographs of the W samples after the exposure to He plasmas under high background pressure conditions (~10^{-4} Pa) with incident ion energies of 350, 200 and 150 eV. Figure 2 shows NTBs were generated on the surfaces and are separated from each other on the surface. When the background pressure was ~10^{-5} Pa (low impurity condition), no NTBs were formed, but general fuzzy nanostructures grew on the entire surface as shown in figure 2(d). It is interesting to note that NTBs growth resulted from just increasing the background pressure to ~10^{-4} Pa without any impurity sources except for those present in the residual air. In this case, the impurity level is assumed to be ~0.04% considering the ratio of background pressure to the operational pressure. Similar surface structures had been developed when a W surface was exposed to a He ion beam containing 0.01% of carbon (C) impurity with an ion energy set at 300 eV [16]. The experiments by *Al-Ajlony et al* used a different impurity species and quantity to the current work, however these results showed explicitly that a very subtle increase in impurity level can lead to significant morphology changes on the W surface.

The NTBs in figures 2(a) and (b) had sharper tips and more irregular structures compared with the shape of NTBs in [11]. By contrast NTBs in figure 2(c) had mainly narrower arch-like structures. Figures 2(e)–(h) show the enlarged micrographs of the boundaries between NTBs and sample surfaces marked in figures 2(a)–(c). Figures 2(e) and (f) show the central regions and the periphery of the surface in figure 2(a), respectively. In figure 2(d) where a low plasma impurity concentration was used, a large covering of fuzzy tendril structure is noticed on the surface. In figures 2(e) and (f) the temperature, ion energy and fluence are very similar to that of figure 2(d) but now an increased plasma impurity concentration has led to the appearance of NTB on the sample. Under the high impurity condition, sputtering and resultant net erosion increases due to the impact of heavier ions than He impacting on the W surface, affecting the fuzz growth. Most of the NTBs were generated on the periphery of the sample where a fuzzy layer was developed as shown in figure 2(f). It is notable that the flux concentration could be enhanced around the edges [17]. This flux enhancement would result in further growth of the fuzz and perhaps NTBs on the periphery as shown in figure 2(a). In this study, the He ions were not magnetized and the ion incident angle was normal to the surface. Thus, it was likely that the incident flux on the interior of the surface was almost uniform. Indeed, the morphology dependence on the axial direction of the plasma column from upstream to downstream was not observed on the interior of samples. Samples with lower incident energies, i.e., 200 and 150 eV, featured surfaces covered with a fuzzy layer as shown in figures 2(g) and (h). It is thought that the decrease in erosion by ion sputtering due to the lower incident ion energy could result in the increase in the effective fuzz thickness [18], and it was noticed that NTBs were also produced across these same sample surfaces. Although only a few

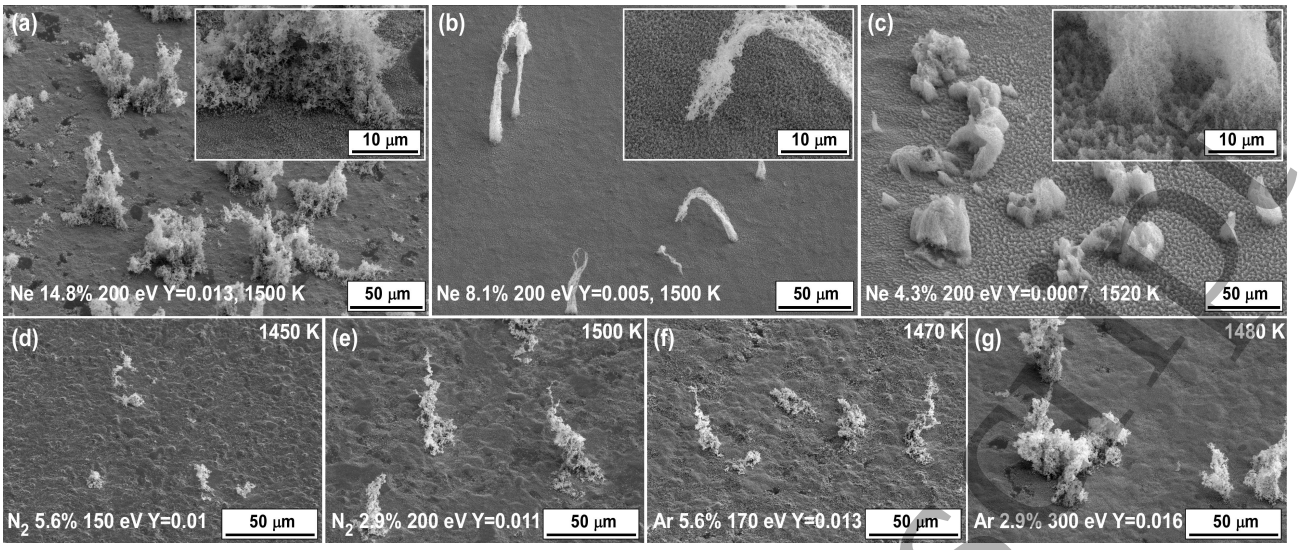

Figure 3. The SEM micrographs of NTBs on W with impurity gas-puffing observed from the viewing angle of 45° from normal. (a)–(c) show the SEM micrographs of NTBs with the same incident ion energy of 200 eV and different Ne gas ratio to He gas: (a) 14.8, (b) 8.1 and (c) 4.3%, respectively, and insets show the enlarged boundaries between NTBs and the surfaces. (d)–(g) shows NTBs with different impurity (N_2 or Ar) ratios and the incident ion energy. The ion fluence was 2×10^{25} m^{-2} for all the samples.

NTBs were observed on non-fuzzy surfaces, mostly NTBs were seen when a fuzzy layer was also observable. Fuzz growth or some He ion-induced morphology change seems to be one of the important contributing factors for NTB formation.

3.2 NTB growth with the injection of impurity gases

Figure 3 shows the micrographs of the samples exposed to He plasmas when secondary gases, such as Ne, N_2 or Ar, were added with the same ion fluence (2×10^{25} m^{-2}). Figures 3(a)–(c) show the NTBs formed with Ne gas injection with the same incident energy of 200 eV. The shapes of NTBs drastically altered with Ne gas ratio variation. Figures 3(a) and (b) had similar structures to those in figure 2(b) and (c), respectively, whereas NTBs in figure 3(c) were more rounded and fuzzy than the others. Figures 3(d)–(g) show NTBs formed with N_2 or Ar gas injection with different incident ion energy and impurity gas ratio. The shapes of NTBs were similar to those in figures 2(a) and (b), or figure 3(a). As discussed later, those morphology changes of NTBs seem to be related to changes in erosion level.

We believe the erosion by ion impact and fuzz growth seems to be linked to the formation of NTBs. Figure 4 shows the formation conditions for NTBs in terms of impurity gas ratio and the incident ion energy for Ne, Ar, N_2 gases and residual air. An inverse relationship between the ion energy and impurity gas ratio to form the NTBs was seen for each impurity gas used, and a lower ion energy boundary for each gas impurity can also be estimated from figure 4. Note that the typical fuzz was developed uniformly on the surface when the ion energy was below the lower limit. The minimum incident ion energy required for NTB formation was in the order of N_2 < Ar < Ne which could be due to the difference in sputtering properties [19]. However, atomic or molecular mass was Ne < N_2 < Ar. it is likely that N_2 works as many different forms, such as multiply charged N ions or N_2 ions. Note that spectroscopy in NAGDIS-II with closing the downstream molecular pump detected band spectra of N_2 molecules as well as N^{2+} line spectra [15]. It has been known that molecular ion impact significantly enhanced the sputtering yield at the ion energy below 1 keV [20, 21]. The sputtering yield per incident N atom by N_2^+ bombardment was 1.2 times higher than that by N^+ at 350 eV [20]. For sputtering of Au, it was found that at ion energies around 50 eV there could be a 4 times higher sputtering yield per incident atom for N_2^+ bombardment compared to N^+ [21]. Therefore the apparent minimum ion energy for NTB production when using N_2 indicated in figure 4 could result from the possible enhancement of sputtering by N_2^+ and N^{2+} ions.

3.3 Influence of erosion and deposition of W to NTB formation

The inverse relation between the incident ion energy and impurity gas ratio in figure 4 indicates that NTB growth has a correlation with a certain

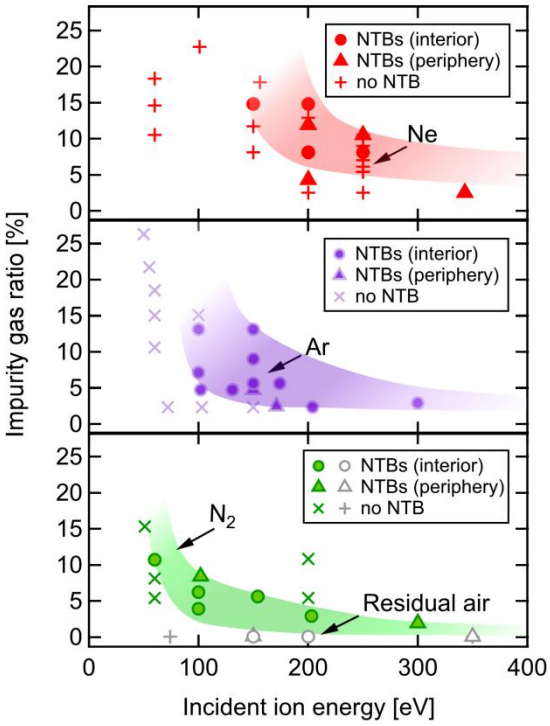

Figure 4. Impurity gas ratio on the vertical axis and the incident ion energy on the horizontal axis for (a) Ne, (b) Ar and (c) N_2 gases. Circle markers represent the cases that the NTBs cover the interior as well as the periphery, while triangle markers represent that NTBs form only on the periphery of the surface. Note that the shaded regions are drawn to guide the eyes.

amount of erosion. Figure 5 shows the formation conditions of NTBs according to the net erosion yield and the target potential. The samples where NTBs were formed on the whole surface and the peripheries were marked as circle and triangle, respectively. Note that uncertainty in the net erosion yield marked in figure 5 was mainly due to uncertainty of ion fluence caused by plasma fluctuation in NAGDIS-II. Typical uncertainty in the mass loss measurement was typically ~0.1% of mass change. To compare the erosion among the gas species, theoretical sputtering yields [19] of singly charged Ar, N, Ne and doubly charged N ions with 10% of impurity ratio, and pure He ions are also shown in figure 5. NTBs were formed when the net erosion yield was in the range of $Y \sim 10^{-3}$–10^{-2} regardless of impurity gas species. Under $Y < 10^{-3}$, erosion and deposition would be overwhelmed by fuzz growth and NTB seems hardly generated as a result.

Woller et al have suggested the possibility of detachment of large-size NTBs which increased the net erosion [11]. In figure 5, most of the data points with NTBs appeared to have greater net erosion yield than the theoretical sputtering yield which was derived with consideration of the impurity gas ratio.

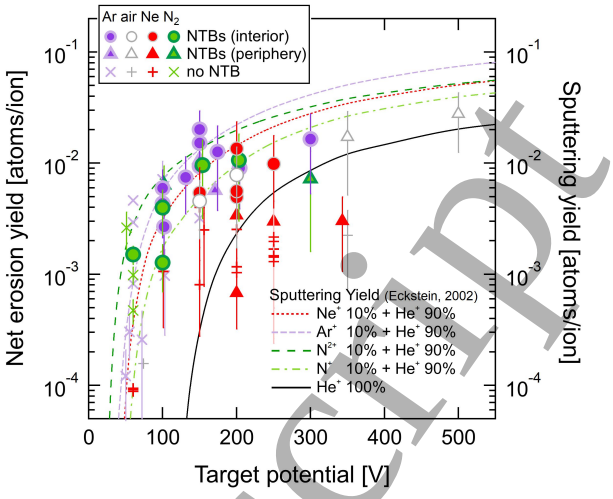

Figure 5. Net erosion yield on the vertical axis and the target potential on the horizontal axis for all the samples. Corresponding sputtering yield were shown with line on the right y-axis. The markers are the same as the ones in figure 4.

The enhanced net erosion might be caused by the detachment of NTBs. On the other hand, for several points for Ne and N_2 impurities, the net erosion yields were below the theoretical sputtering curve. In this case, the decrease in the sputtering yield is believed to be because of line-of-sight deposition of sputtered W atoms on to the fuzz tendrils themselves [22]. Hence for these cases it is apparent that increased erosion by NTB detachment would be hardly distinguished.

As shown in figure 4, there appears to be some correlation between the impurity level and the incident ion energy in the onset of NTB formation. The net erosion yields would increase as the two parameters increase, hence it is difficult to say that the enhanced net erosion and the NTB growth is necessarily in a cause-effect relationship. However, recalling the inverse relationship between the two parameters implies the existence of a sputtering-erosion window for NTB growth; from the current work a net erosion yield range of 10^{-2}-10^{-3} seems to be necessary for NTB formation.

For NTBs with sharper tips and irregular structures (figure 2(b) and figures 3(a), (d)–(g)), the net erosion yields were in the range of $Y \sim$ 0.008–0.016. Conversely, NTBs with arch or needle-like structures (figure 2(c) and figure 3(b)) had $Y \sim 0.005$. NTBs with more rounded surface (figure 3(c)) had much lower net erosion yield of $Y \sim$ 0.0007. Even with the similar erosion yield, the size of NTBs were different with the impurity gas ratio. In figures 3(d)–(g), NTBs tend to become greater in size as the impurity gas ratio decreases. Considering that

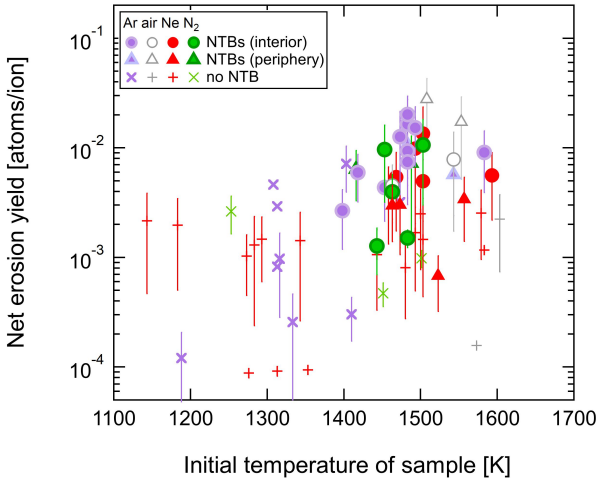

Figure 6. Net erosion yield on the vertical axis and the sample temperature at the initial stage of plasma irradiation on the horizontal axis for all the samples. The markers are the same as the ones in figure 4 and 5.

the ion fluence was the same and that the W surface did not change with pure impurity ion exposure [23], the increased He ions would activate morphology change more on the W surface resulting in further growth of NTBs.

3.4 Sample temperature dependence

Figure 6 shows the dependence of NTB formation on the sample temperature at the initial stage of plasma irradiation and the net erosion. The NTBs grew up at the temperature in the range of 1400-1600 K, which was beyond the upper limit of the NTB formation window (1020-1220 K) in [11]. NTBs grew entirely across the surface when the surface temperature was in the range of 1400-1500 K, while most samples had a few or no NTB on the surface above 1500 K. Figure 7 shows SEM micrographs of two samples exposed to the Ne mixed plasma with different surface temperatures. The number of NTBs at 1590 K was fewer than that at 1500 K. As shown in figure 7(a), at a higher surface temperature (~1590 K), recrystallised grains were dominant in the surface morphology with a few initial nanoscale protrusions, whereas nanostructured fuzz fully covered the surface in figure 7(b) at a lower temperature of 1500 K. From [24], it is clear that some level of annealing of fuzzy structures occurs as surface temperature increases. In this work it is likely that annealing due to increased temperatures from 1500 to 1590 K in figure 7 has resulted in a lower growth rate of typical fuzz and NTB structures.

The temperature window for NTB formation does not overlap the previous conditions in [11].

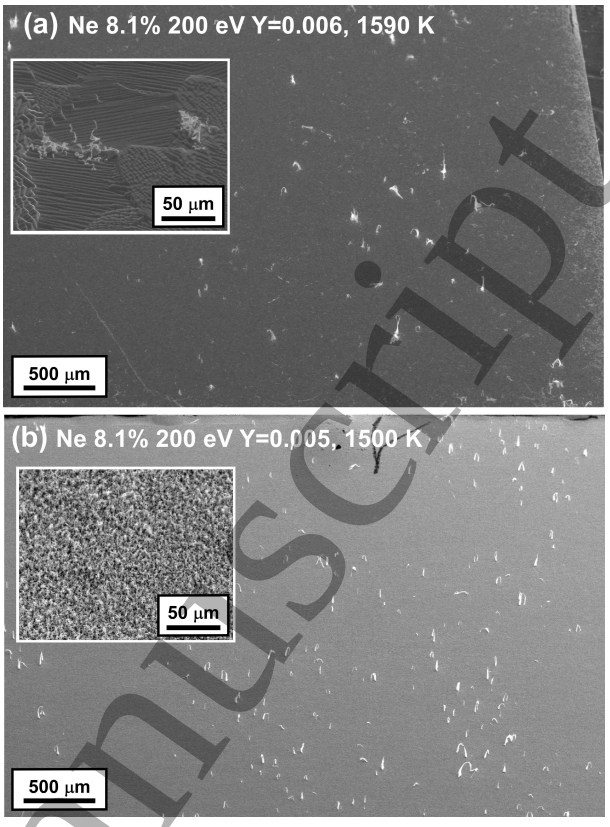

Figure 7. The SEM micrographs of NTBs on W with neon gas-puffing viewed from 45° to the surface normal with the same incident ion energy and neon gas ratio of 200 eV and 8.1%, respectively, and with different surface temperature: (a) 1590 and (b) 1500 K, respectively. The insets show the enlarged surface morphologies of the sample plane.

There still exists a possibility for NTB growth at a lower temperature. It is known that the measured surface temperature decreases when fuzzy nanostructures form causing an emissivity increase from the surface. For a fully grown fuzzy surface, the measured temperature can be decreased by ~300 K [25, 26]. In the present paper, the growth of fuzzy layer would be saturated due to significant erosion by impurity and He ions, as predicted in [27]. The vast majority of sample surfaces with NTBs had thin layers with loop-like protrusions of several hundreds of nm, except for the exceptional case with Ne mixture as shown in figure 3(c), and the surface colors visible with the naked eye were not black but gray or silver. Considering the required He fluence for the fuzz growth in this scale [27] and the corresponding emissivity change [26], it was likely that the expected temperature decreases in this paper did not exceed 150 K. Nevertheless, it is implied that the initial growth of NTB could start at lower temperature range than the measured initial temperatures.

In this work, the surface temperature was controlled by shifting the position of samples from the plasma center resulting in a change in ion flux, hence the amount of heating supplied by the incident ion flux was also altered. Growth speed of fuzz saturates when ion flux exceeds a certain value [28], and that value can vary with experimental conditions. If the growth of NTB is affected by the formation of nanoscale protrusions or fuzzy layers, as mentioned in section 3.1, the flux difference can also have influence on the NTB formation. One can notice that some amount of net erosion is also required even when the temperature is above 1400 K. For a future investigation, a temperature range which overlaps the values of the previous report [11] and high net erosion near $Y \sim 0.01$ should be surveyed to explore a clearer and more coherent formation window for NTB's.

3.5 Potential NTB growth mechanism

A mechanism for NTB growth is still unclear. A discrepancy in the experimental conditions existed between the present and the previous result. In this section, a comparison is made between two experimental cases to speculate the growth mechanism of NTB's. The growth mechanism may have both intrinsic and extrinsic aspects. Regarding the former one, *Woller et al* have presented the effect of RF modulation of plasma using the range of 30–100 eV of RF modulated plasma [11]. In RF frequency regime, typical fuzz growth was mitigated but NTBs formed instead. The NTB formation was observed even without using RF modulated biasing [29]. It was revealed that RF bias modulation is not a prerequisite for NTB growth, but ion energy spread with ~70 eV of ion energy distribution width is required to form NTBs. With comparatively narrow ion energy width of ~24 eV, typical W fuzz was developed [29]. Based on the experimental results, they have discussed about the diffusion distance of implanted He in W and the characteristic distance travelled by W adatoms with regards to the RF time scale, making it conceivable that the ion energy modulation could affect the intrinsic kinetics of He bubbles and surface adatoms.

In the present work, however, both plasma source and sample biasing were performed as DC, making it difficult to expect the same effect as the RF ion modulation did in [11, 29]. In addition, in [29] *Woller et al* have mentioned that NTBs were also formed when the modulation frequency was 20 kHz, which was reduced by a factor of ~1000, making it unlikely that the RF modulation effects on W adatom travel on the RF time scale affected the intrinsic kinetics of W surface. Instead, the extrinsic effects can be explicit in the present condition. As mentioned above, some level of net erosion was correlated with NTB growth. If the level of re-deposition is changed according to the net erosion level, then this result indicates that NTB growth can be formed by extrinsic erosion and deposition of W as well as by sub-surface kinetics evoked using the RF modulation. To further explore the growth process of NTBs, the difference in the sputtering at W surface grains can be considered. One can notice from the smooth (dark) surfaces in figures 2(e), in comparison with figure 2(h) and figure 3(a), that grain orientation dependence of fuzz growth [30] would be maximized under a sputtering regime because once the surface starts to become fuzzy the sputtering yield would decrease on that surface [19]. If the fuzz starts to preferentially grow on certain grains, it is likely that these areas where fuzz has been shown to grow at an accelerated rate can be nuclei for deposited W particles due to the line-of-sight deposition effect seen in [22]. This would result in an enhanced morphology changes on those particular regions. Recently, large-scale, on the order of mm, fuzz growth was resulted from precipitating additional W particles onto a W substrate [31]. The large scale of fuzzy structure started to grow from protruding area prior to the other smooth area, and the fuzz morphology accompanied by He bubble growth was likely to be a prerequisite for enhanced fuzz growth. These results are consistent with the findings in the current work and indicate that initial growth phase of nanostructuring should be handled delicately especially under the deposition-induced NTB growth environment. It is notable that in [31] the bundles of fuzz nanowires developed to membranes, and the membrane structures were also found on some surfaces of this work. This also supports the idea that the present work and the work in [31] possibly share a similar growth mechanism. In addition, one can consider the enhancement of the displacement damage of tungsten by impurity ion bombardment which enables to create more vacancies and, as a result, enhances trapping or nucleation of He under the target surface. Thus, it is likely that the impurity ions and the resulting erosion effect are one of the prerequisites for NTB formation. For a comprehensive understanding of the NTB growth mechanism, it would be helpful to introduce both the ion energy modulation effect and the erosion and deposition effect caused by impurity ion bombardment simultaneously.

It is useful to note that the impurity concentration required for plasma detachment in future fusion devices such as ITER and DEMO is

expected to be in the range of ~1–2% for Ar or Ne [12, 13]. That is, the He to impurity ratio would be similar to this research considering the ratio of He density to the electron density of core plasma is not expected to exceed 10% [32, 33]. In addition, at the outer region from the strike point of the outer target of the W divertor, the incident ion energy can reach ~250 eV [34], which may lead to significant erosion of these regions. This high energy ion flux, made up of He and impurity species, could result in the growth of NTBs through ionization and re-deposition of the eroded W.

4. Conclusion

In this paper, it is demonstrated that nano-tendril bundles can be formed on tungsten surfaces by DC He plasma exposure with impurity gases, such as Ne, Ar, N_2 and residual air. In comparison to previous results by *Woller et al*, NTBs could grow without RF modulation, but a certain level of net erosion was featured with a formation window of net erosion yield (*Y)* around 10^{-3}–10^{-2}. NTBs were formed by just increasing the background pressure from ~10^{-5} to ~10^{-4} Pa without secondary gas addition. The shapes of NTBs varied with exposure condition, depending mainly on the net erosion yield. The required impurity gas ratio for NTB formation was different depending on the gas species, likely due to the difference in sputtering ability. By having impurity gas present in the He plasma, it is shown that NTBs are produced. Considering ~10% of impurity gas ratio to He gas in this research, it is probable that NTBs can also be formed in future fusion devices where W divertor and impurity gas seeding are expected to be used and high energy transient events such as ELMs may occur.

Acknowledgments

The authors would like to thank Prof. N. Yoshida at Kyushu University for fruitful discussion. This work was supported in part by JSPS KAKENHI 15H04229 and NIFS/NINS under the project of Formation of International Network for Scientific Collaborations. P. McCarthy would like to acknowledge the Engineering and Physical Sciences Research Council [grant ref. EP/L01663X/1] for supporting this work.

References

[1] Loarte A et al 2007 *Nuclear Fusion* **47** S203–63
[2] Pitts R A et al 2013 *Journal of Nuclear Materials* **438** S48–56
[3] Iwakiri H, Yasunaga K, Morishita K and Yoshida N 2000 *Journal of nuclear materials* **283** 1134–1138
[4] Takamura S, Ohno N, Nishijima D and Kajita S 2006 *Plasma and fusion research* **1** 051–051
[5] Baldwin M J and Doerner R P 2008 *Nuclear Fusion* **48** 035001
[6] Kajita S, Sakaguchi W, Ohno N, Yoshida N and Saeki T 2009 *Nuclear Fusion* **49** 095005
[7] Kajita S, Yagi T, Kobayashi K, Tokitani M and Ohno N 2016 *Results in Physics* **6** 877–8
[8] Kajita S, Ohno N, Hirahata Y and Hiramatsu M 2013 *Fusion Engineering and Design* **88** 2842–7
[9] Hwangbo D, Kajita S, Ohno N and Sinelnikov D 2017 *IEEE Transactions on Plasma Science* **45** 2080–6
[10] Sato D, Ohno N, Domon F, Kajita S, Kikuchi Y and Sakuma I 2017 *Nuclear Fusion* **57** 066028
[11] Woller K B, Whyte D G and Wright G M 2017 *Nuclear Fusion* **57** 066005
[12] Pacher G W, Pacher H D, Janeschitz G, Kukushkin A S, Kotov V and Reiter D 2007 *Nuclear Fusion* **47** 469–78
[13] Wenninger R et al 2015 Advances in the physics basis for the European DEMO design *Nuclear Fusion* **55** 063003
[14] Ohno N, Nishijima D, Takamura S, Uesugi Y, Motoyama M, Hattori N, Arakawa H, Ezumi N, Krasheninnikov S, Pigarov A and others 2001 *Nuclear fusion* **41** 1055
[15] Hwangbo D, Kawaguchi S, Kajita S and Ohno N 2017 *Nuclear Materials and Energy* **12** 386-391
[16] Al-Ajlony A, Tripathi J K and Hassanein A 2015 *Journal of Nuclear Materials* **466** 569-575
[17] Baldwin M J, Dejarnac R, Komm M and Doerner R P 2017 *Plasma Physics and Controlled Fusion* **59** 064006
[18] Noiri Y, Kajita S and Ohno N 2015 *Journal of Nuclear Materials* **463** 285–8
[19] Eckstein W 2002 Calculated Sputtering, Reflection and Range Values vol.9 (Germany: Garching)
[20] Dobes K, Naderer P, Lachaud N, Eisenmenger-Sittner C and Aumayr F 2011 *Physica Scripta* **T145** 014017
[21] Yao Y et al 1998 *Physical Review Letters* **81** 550
[22] Nishijima D, Baldwin M J, Doerner R P and Yu J H 2011 *Journal of Nuclear Materials* **415** S96–9
[23] Yajima M, Yamagiwa M, Kajita S, Ohno N, Tokitani M, Takayama A, Seiki Saito, Ito A M, Nakamura H and Yoshida N 2013 Plasmas *Plasma Science and Technology* **15** 282
[24] Kajita S, Ohno N, Yajima M and Kato J 2013 *Journal of Nuclear Materials* **440** 55-62
[25] Takamura S, Miyamoto T and Ohno N 2013 *Journal of Nuclear Materials* **438** S814–7
[26] Kajita S, Yokochi T, Ohno N and Kumano T 2012 *Japanese Journal of Applied Physics* **51** 01AJ03
[27] Petty T J, Baldwin M J, Hasan M I, Doerner R P and Bradley J W 2015 *Nuclear Fusion* **55** 093033

[28] Baldwin M J, Doerner R P, Nishijima D, Tokunaga K and Ueda Y 2009 *Journal of Nuclear Materials* **390-391** 886-890
[29] Woller K B, Whyte D G, Wright G M 2017 Nuclear Materials and Energy **12** 1282-1287
[30] Ohno N, Hirahata Y, Yamagiwa M, Kajita S, Takagi M, Yoshida N, Yoshihara R, Tokunaga T and Tokitani M 2013 *Journal of Nuclear Materials* **438** S879–82
[31] Kajita S, Kawaguchi S, Ohno N and Yoshida N 2018 *Scientific Reports* **8** 56
[32] Kukushkin A 2008 ITER Report [ITER_D_27TKC6]
[33] Pacher G W, Pacher H D, Janeschitz G, Kukushkin A S, Kotov V and Reiter D 2007 *Nuclear Fusion* **47** 469–78
[34] Hoshino K, Asakura N, Tokunaga S, Homma Y, Shimizu K, Sakamoto Y and Tobita K 2017 *Fusion Engineering and Design* **124** 352-355